

Neutronics and burnup analysis of VVER-1000 LEU and MOX assembly computational benchmark using OpenMC Code

Md. Imtiaz Hossain¹, Yasmin Akter¹, Mehrnaz Zaman Fardin¹, Abdus Sattar Mollah¹

¹ Department of Nuclear Science & Engineering, Military Institute of Science and Technology, Dhaka, Bangladesh

Corresponding author: Abdus Sattar Mollah (mosattar54@gmail.com)

Academic editor: Georgy Tikhomirov ♦ **Received** 25 November 2021 ♦ **Accepted** 22 February 2022 ♦ **Published** 14 March 2022

Citation: Hossain MdI, Akter Y, Fardin MZ, Mollah AS (2022) Neutronics and burnup analysis of VVER-1000 LEU and MOX assembly computational benchmark using OpenMC Code. Nuclear Energy and Technology 8(1): 1–11. <https://doi.org/10.3897/nucet.8.78447>

Abstract

A handful of computational benchmarks that incorporate VVER-1000 assemblies having low enriched uranium (LEU) and the mixed oxide (MOX) fuel have been put forward by many experts across the world from the Nuclear Energy Agency. To study & scrutinize the characteristics of one of the VVER-1000 LEU & MOX assembly benchmarks in different states were considered. In this work, the VVER-1000 LEU and MOX Assembly computational-benchmark exercises are performed using the OpenMC software. The work was intended to test the preciseness of the OpenMC Monte Carlo code using nuclear data library ENDF/B-VII.1, against a handful of previously obtained solutions with other computer codes. The k_{inf} value obtained was compared with the SERPENT and MCNP result, which presented a very good similarity with very few deviations. The k_{inf} variation with respect to burnup upto 40 MWd/kgHM was obtained for State-5 by using OpenMC code for both the LEU and MOX fuel assembly. The depletion curves of isotope concentrations against burnup upto 40 MWd/kg/HM were also generated for both the LEU and MOX fuel assembly. The OpenMC results are comparable with those of benchmark mean values. The neutron energy vs flux spectrum was also generated by using OpenMC code. Based on the OpenMC results such as k_{inf} , burnup, isotope concentrations and neutron energy spectrum, it is concluded that the OPenMC code with ENDF/B-VII.1 nuclear data library was successfully implemented. It is planned to use OpenMC code for calculation of neutronics and burnup of the VVER-1200 reactor to be commissioned in Bangladesh by 2023/2024.

Keywords

VVER-1000, OpenMC, multiplication factor, burnup, isotope concentrations, Light Enriched Uranium (LEU) Assembly, Mixed Oxide (MOX) fuel Assembly, Benchmark

Introduction

The main purpose of nuclear reactor theory is calculation of distribution of neutrons in the reactor core. From knowledge of it, we can determine the rate of fission reaction occurring in a nuclear reactor and hence reactor power and operating point (sub critical, critical or supercritical) hence, stability of fission chain reaction can

be inferred. Generally, neutronic analysis is performed based on “Deterministic” and “Stochastic” methods. In deterministic methods the transport equation is solved as a differential equation. In stochastic methods such as Monte Carlo, discrete particle histories are tracked and averaged in a random walk directed by interaction probabilities. In Bangladesh, two Russian design VVER-1200 (2400 MWth) type nuclear reactors are under

construction and to be commissioned by 2023/2024. A program has been undertaken at the Department of Nuclear Science and Engineering of Military Institute of Science and Technology, Dhaka, Bangladesh to introduce some Monte Carlo computer codes such as MCNPX (Louis and Amin 2016), SERPENT (Mercatali et al. 2021), SuperMC (Wu et al. 2015), and OpenMC (Romano et al. 2015) Romano and Forget 2013) for neutronics calculations of different types of nuclear reactors. As a part of this program, the OpenMC code has been adopted to perform neutronics analysis of benchmark problems for two types of fuel assembly (LEU and MOX) that are typically of the advanced Russian designs. Benchmarks are specified problems used to test nuclear data libraries & validate computer codes (Alhassan et al. 2014). These act as a learning tool for engineers that enable them to perform neutronic calculations for various types of nuclear reactors. To ease the sharing of prevailing information & intelligence about the forthcoming designs of VVER-1000 LEU & MOX fuel, a VVER-1000 LEU & MOX fuel assembly computational benchmark was put forward by a group of professionals at OECD/NEA (OECD NEA 2002). The benchmark was analyzed using six codes obtained from five institutions, of which two were developed using continuous energy Monte Carlo method, i.e. MCNP-4B & MCU & for the rest, the collision probability method was used. The average values obtained from these codes are denominated as “Benchmark Mean” which is mentioned below in the result section. Additionally, the same problem was analyzed using various codes & data libraries over the past several years. Some of them are EXCEL (Thilagam 2009), APOLLO2 & TRIPOLI4 (Petrov 2013), MCNPX (Louis and Amin 2016), VISWAM (Khan et al. 2016) & GETERA (Abuqudaira and Stogov 2018). Having been launched in December 2012, OpenMC is a fairly new Monte Carlo-particle transport code (Romano and Forget 2013) which gives the user an advantage of obtaining results based on the average result of three different methods namely track length, collision probability & absorption. One can also use the results obtained from any individual method instead of the average one. In this study, ENDF/B-VII.1 was used. ENDF/B-VII.1 is an evaluated nuclear data library that contains all necessary cross-section data to perform a neutronic analysis. This library has nuclear data for 423 nuclides (ENDF/B-VII.1 2012). The work is intended to perform neutronic, burnup and isotope concentrations analysis of the VVER-1000 computational benchmark using OpenMC code.

Benchmark description

The benchmark model has two fuel assemblies (LEU & MOX) of the VVER-1000 reactor. Each of the assemblies consists of 331 elementary cells of four types for LEU assembly & six types for MOX assembly inside a hexagonal lattice. Twelve Gd_2O_3 pins are located inside each

assembly as a burnable absorber at completely different positions. The layout of both the assembly types obtained using OpenMC is shown in Figs 1 and 2. The assembly has a uniform enrichment of 3.7% in ^{235}U except in Gd, bearing pins that contain 3.6% wt. of ^{235}U and 4% wt. of Gd_2O_3 . The assembly lattice pitch & the hexagonal cell pitch are respectively 23.6 cm & 1.275 cm. All three types of unit cells along with their dimensions for each assembly are given in Figs 1 and 2. The cladding and structural materials are of a Zircaloy. Both material & geometry specifications used in the assemblies are taken from the benchmark report (OECD NEA 2002).

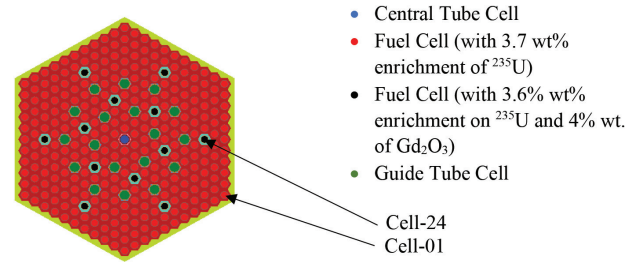


Figure 1. LEU fuel assembly.

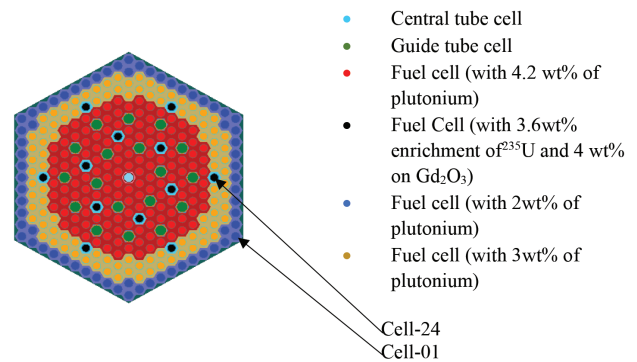


Figure 2. MOX fuel assembly.

Geometry description

The cell type geometry specifications are given in Table 1. The fuel and non-fuel cells are shown in Fig. 3.

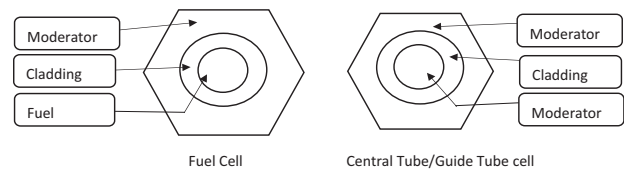


Figure 3. Fuel & non-fuel cells.

Table 1. Cell type geometry specification

Type of the Cell	Cell Radius (in cm)
Fuel	Fuel pellet radius = 0.386
	Cladding outer radius = 0.4582
	Cladding inner radius = 0.545
Guide tube cell	Cladding outer radius = 0.6323
	Cladding inner radius = 0.48
Central tube cell	Cladding inner radius = 0.48
	Cladding outer radius = 0.5626

Table 2. Reactor States for both of the assembly

State	State name	Fuel temperature in K	Non-fuel temperature in K	Boron concentration (ppm)	¹⁴⁹ Sm ¹³⁵ Xe	Moderator in fuel & central/guide tube	Moderator density in g/cm ³
State 1	Operating poisoned state	1027	575	600	Eq.	MOD1	0.7235
State 2	Operating non-poisoned state	1027	575	600	0	MOD1	0.7235
State 3	Hot state	575	575	600	0	MOD1	0.7235
State 4	Hot state without boric acid	575	575	0	0	MOD2	0.7235
State 5	Cold state	300	300	0	0	MOD3	1.0033

Methodology

The models were represented in the OpenMC using python (python 3.7) code in Jupyter notebook. Initially, one of each of the different types of rods was created. To obtain the assemblies, they were placed in a hexagonal lattice with a lattice cell pitch of 1.275 cm and an assembly pitch of 23.6 cm. Modeling was done utilizing Boolean operations to define different zones within the cells. The hexagonal lattice and two different planes in the z-axis with reflecting boundary conditions bounded the geometry, which is equivalent to the geometry being infinite in the z-axis. For thermal scattering at low energies, S(α,β) table was used. The benchmark demands a solution for a variety of states, encompassing both hot and cold conditions, as shown in Table 2. Assumptions taken during the OpenMC process are:

- Pin-by-pin Model
- Reflective boundary condition in all directions (x, y & z)
- Finite boundary at z-axis with reflective boundary conditions.
- Cross-section data library: ENDF/B-VII.1
- 1000 batches with 100 inactive batches & 11000 particles in each batch.

In OpenMC code, there are three ways to calculate k -eigenvalue, including track-length estimator, collision estimator, and absorption estimator, respectively. They are expressed in the following equations:

$$k_{\text{track-length}} = \frac{\sum_{\text{all flights}} w_j d_j \nu \Sigma_f}{W}$$

$$k_{\text{Collision}} = \frac{\sum_{\text{all collisions}} w_j \left(\frac{\nu \Sigma_f}{\Sigma_t} \right)}{W}$$

$$k_{\text{track-length}} = \frac{\sum_{\text{all absorption}} w_j \left(\frac{\nu \Sigma_f}{\Sigma_a} \right)}{W}$$

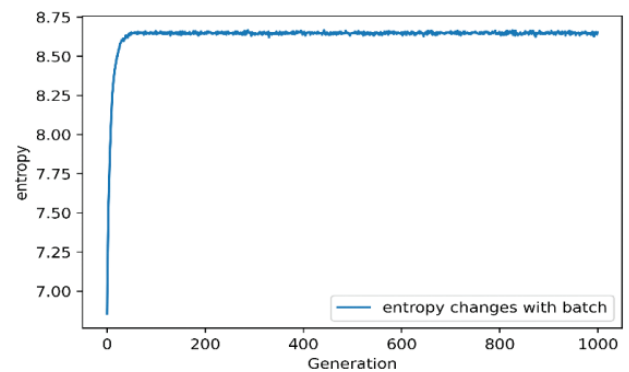
where W is the total weight starting each generation (or batch), w_j is the pre-collision weight of the particle as it enters event j , d_j is the length of the j^{th} trajectory, and $\nu \Sigma_f$ and Σ_a are macroscopic neutron production cross section and absorption cross section.

The OpenMC Monte Carlo code was used to calculate the average k_{inf} based on the combined collision estimator, track length estimator, & absorption estimator (Wu et al. 2015).

Results and discussion

Infinite multiplication factor

The infinite multiplication factor was calculated in eigenvalue mode of the OpenMC (Version 0.12.2) monte carlo code. To obtain accurate results based on the initial guess value for the fission source distribution, analysis of the iteration method source convergence is necessary. A study into convergence of Monte Carlo criticality analysis has proved that the Shannon entropy of the fission source distribution, H_{src} , is an effective parameter for identifying the convergence of the fission source distribution (Brown 2006). The OpenMC monte carlo code includes new tools for determination and plotting of Shannon entropy of the fission source distribution to assess problem convergence. To ensure that the result converges, the Shannon entropy was measured at zero burnups, and an approximation of the inactive batches was determined. The Shannon entropy versus generation curve as shown in Fig. 4, aids in determining the number of inactive batches. The number of inactive batches is taken to be 100, before which the entropy curve starts showing constant behavior.

**Figure 4.** Shannon entropy vs generation.

The OpenMC results of the present study were compared to the results of SERPENT code as well as the MCNP results (Mercatali et al. 2015). The k_{inf} values obtained by using OpenMC code are given in Tables 3 and 4 at zero burnup for both LEU and MOX fuel assembly, respectively. Tables 3 and 4 reveal that OpenMC and other

Table 3. k_{inf} for Zero burnup (For LEU)

LEU	SERPENT(SE) (ENDF/B-VII.0)	OpenMC (OP) (ENDF/B-VII.1)	MCNP (JEFF 2.2)	ΔK (OP-SE)* 10^5
State 1	1.13997 \pm 8.8E-05	1.13923 \pm 2E-04	-	-74
State 2	1.17587 \pm 8.8E-05	1.17520 \pm 2E-04	1.1800 \pm 6E-05	-67
State 3	1.18996 \pm 8.6E05	1.18849 \pm 2E-04	1.1925 \pm 6E-05	-147
State 4	1.24993 \pm 8.7E05	1.24896 \pm 2.5E-04	1.2531 \pm 7E-05	-97
State 5	1.32305 \pm 7.7E05	1.32210 \pm 2E-04	1.3235 \pm 6E-05	-95

Table 4. k_{inf} for at Zero burnup (for MOX fuel)

MOX	SERPENT(SE) (ENDF/B-VII.0)	OpenMC (OP) (ENDF/B-VII.1)	MCNP (JEFF 2.2)	ΔK (OP-SE)* 10^5
State 1	1.17382 \pm 8.4E-05	1.17131 \pm 1.8E-04	-	-51
State 2	1.19762 \pm 8.6E-05	1.19740 \pm 1.8E-04	1.1922 \pm 7E-05	-22
State 3	1.21429 \pm 8.4E-05	1.21378 \pm 1.8E-04	1.2091 \pm 6E-05	-51
State 4	1.24923 \pm 8.4E-05	1.24822 \pm 1.8E-04	1.2430 \pm 6E-05	-99
State 5	1.33013 \pm 7.6E-05	1.33033 \pm 1.8E-04	1.3256 \pm 6E-05	20

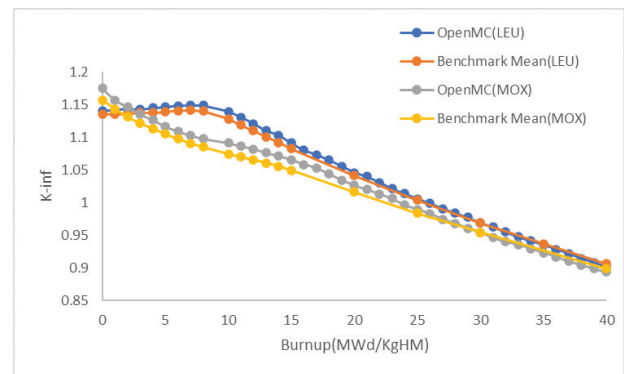
codes (such as SERPENT and MCNP) have a high degree of similarity in terms of nature and value.

Table 3 compares the infinite multiplication factor computed by OpenMC with ENDF/B-VII.1 nuclear data library with those of the literature values obtained from SERPENT code using ENDF/B-VII nuclear data library at zero burnup for LEU fuel assembly, and shows that OpenMC and SERPENT agree quite well in case of LEU fuel assembly. As demonstrated in Table 3, there is a little variation due to the use of different nuclear data libraries. The comparison of these two nuclear data libraries can help explain the causes. In the case of MOX fuel assembly (Table 4), the OpenMC results are comparable with those of the results obtained from SERPENT code. Using PREPRO code (Diop et al. 2007), a detailed comparison was done between the two libraries. In ENDF/B-VII.1, there were around 170 variations, with 120 of them differing by 1% or more of total cross-sections from the same isotope in ENDF/B-VII.0. Because these methods utilized various different data libraries such as ENDF/B-VI.0, JEFF2.2, JEFF 3.1, JENDL 3.2, ENDF/B-VII.0, etc., the result differs even more from those shown in benchmark problem & benchmark mean results. Another explanation is that neutron data for fuel material, non-fuel material, and the $S(\alpha, \beta)$ table was used for 579 K instead of 575 K for S2–S4 states due to the unavailability of data at these two temperatures. Table 5 shows a comparison of different results achieved by different codes for the cold state (State-5) for LEU and MOX fuel assembly. The JEFF 3.3 nuclear data library was also used in the OpenMC code to calculate the k_{inf} for the State-5 only (Table 5). The difference between the maximum and the minimum k_{inf} value for the same state is roughly 680 pcm for LEU

and about 1695 pcm for MOX fuel, according to the table. All of the values for the various codes were collected from various sources that are cited in the references. We can conclude from this comparison that the OpenMC results are acceptable.

Burnup effects

The variation of k_{inf} with respect to burnup (MWd/kgHM) is shown in Fig. 5 for LEU and MOX fuel assembly, respectively for State-1. The time burup steps were considered upto 10 MWd/kgHM to model Gd depletion accurately. The S1 state was followed upto 40 MWd/kgHM using the power density 108 MW/m³ given in the benchmark problem. The benchmark values are also included in Fig. 5 for comparison purposes. At burnup of 8 MWd/kgHM the peak value of k_{inf} is seen in Fig. 5 for LEU fuel assembly. In the case of MOX fuel assembly, the peak value of k_{inf} is observed at burnup of ~10 MWd/kgHM. The OpenMC results for the both LEU and MOX fuel assembly are comparable with those of benchmark mean values.

**Figure 5.** Variation of k_{inf} vs burnup**Table 5.** Comparison of different results (State-5)

NAME (Data library)	LEU	MOX
SERPENT(JEFF3.1)	1.32088	1.32908
OpenMC(JEFF3.3) (Present study)	1.31670	1.3297
SCALE(ENDF/B-VII.0)	1.31770	1.32652
MCNP4B(JEFF2.2)	1.3235	1.3256
GETERA(BNAB-93)	1.3175	1.31213

Reactivity effects

The reactivity effect was computed using the k_{inf} values obtained from various reactor operational states at zero burnup for LEU and MOX fuel assembly is given in

Table 6. Reactivity effects (at zero burnup for LEU fuel)

Initial state	final state	Effect	$(K_{init.} - K_{fn.}) / (K_{init.} * K_{fn.}) * 1000$ (mk)			
			OpenMC	Benchmark mean	SERPENT	(OP-SE)
State 1	State 2 effect on reactivity	¹³⁵ Xe & ¹⁴⁹ Sm	-26.30	-30.22	-26.78	-0.48
State 2	State 3	Fuel temperature (Doppler effect)	-9.43	-09.86	-10.07	+0.64
State 3	State 4	Soluble boron effect	-40.18	-40.23	-40.31	+0.13
State 4	State 5	Moderator temperature effect	-44.00	-41.73	-44.21	+0.21

Table 7. Reactivity effects (at zero Burnup for MOX fuel)

Initial state	final state	Effect	$(K_{init.} - K_{fn.}) / (K_{init.} * K_{fn.}) * 1000$ (mk)			
			OpenMC	Benchmark mean	SERPENT	(OP-SE)
State 1	State 2	¹³⁵ Xe & ¹⁴⁹ Sm effect on reactivity	-23.31	-24.15	-23.89	-0.58
State 2	State 3	Fuel temperature (Doppler)	-11.04	-12.21	-11.39	+0.35
State 3	State 4	Soluble Boron	-23.43	-23.19	-23.10	-0.33
State 4	State 5	Moderator Temperature	-49.44	-47.95	-48.69	-0.75

Tables 6 and 7. The OpenMC reactivity values are comparable with those of benchmark mean value including SERPENT value (Mercatali et al. 2015).

Isotopic composition changes with burnup

Figs 6–22 exhibits the results of various radionuclide concentrations for LEU and MOX fuel assembly with respect to burnup for the operating poisoned condition (S1). Predictor Integrator, a first-order predictor algorithm, was employed for depletion analysis. The concentration of neutron poisons Xe-135 and Sm-149 must be in equilibrium for state-1, which is an operating poisoned state. The main difference between State-1 and State-2 is that the former requires the xenon concentration and neutron flux to remain in equilibrium, whereas the latter does not. The purpose of building this forced equilibrium before running the simulation is to account for the xenon oscillation that occurs during a depletion analysis which has a significant impact on the reactivity (Isotalo et al. 2013). Burnup calculation is carried out for this state only.

Isotopic composition changes of nuclides ²³⁵U, ²³⁶U, ²³⁸U, ²³⁹Pu, ²⁴⁰Pu, ²⁴¹Pu, ²⁴²Pu, and ¹⁴⁹Sm in cell-1 and cell-24 (as shown in Figs 2 and 3) of the LEU and MOX fuel assembly as a function of burnup is depicted in Figs 6–22. These changes were obtained from burnup calculation in State-1 which is compared with the Benchmark mean value. In addition, for both the LEU and MOX fuel assemblies, two additional isotopes, ¹⁵⁵Gd and ¹⁵⁷Gd, are compared in cell-24. Because of its large thermal fission cross-section of approx. 583 barns, U-235 is used as the primary fuel in an LEU fuel assembly. As the fission process progresses and burnup increases, the concentration of U-235 in LEU assembly falls. Because Pu is the major fuel in MOX assembly, ²³⁹Pu shows similar behavior which can be seen from Fig. 8 below. In an LEU assembly, all U-235 atoms do not cause fission. Radiative capture yields U-236 in a small fraction of U-235, hence the concentration of U-236 rises with burnup. The same goes for the MOX assembly since it also contains U-235 along with Pu. Despite the fact that U-238 makes up the majority of

the fuel element material in an LEU assembly, its overall fission cross-section is too low compared to that of U-235. However, due to its fast fission & thermal fission (very small amount) and radiative capture, the concentration of U-238 drops as burnup increases. By radiative capture of neutrons, the fertile atom U-238 generates U-239 in an LEU assembly. U-239 quickly emits a beta particle to transform into Np-239 and Np-239, in turn, releases a beta particle to transform into Pu-239, which is relatively stable. Thus, the concentration of Pu-239 increases with burnup in LEU assembly. And in MOX assembly, since the main fuel is Pu-239, as burnup increases the fuel gets used up and its concentration decreases. In an LEU assembly, initially, there's no existence of Pu-240, but as the burnup increases, its concentration also builds due to the neutron capture of previously generated Pu-239. In MOX assembly, the concentration of Pu-240 rises by a large margin with the increase of burnup because the radiative capture of neutrons by U-238 produces Pu-240 after subsequent beta decays. By neutron capture, some Pu-240 nuclei may in turn form Pu-241. In both the LEU and MOX assemblies, the concentration of Pu-241 rises in a similar manner to that of Pu-240. But in LEU assembly, Pu-241 just takes a little longer to grow its concentration as Pu-239 does not exist in this assembly. Pu-242 comes into being when due to the neutron capture of Pu-241. Since neither of the two assemblies had an initial concentration of Pu-242, variation of Pu-242 concentration with burnup in both the LEU and MOX assemblies indicates a similar scenario. However, because of the presence of Pu-241 in the MOX core, the concentration of Pu-242 in MOX assembly rises earlier and is greater than that of LEU assembly. The thermal neutron absorption cross-sections of Gd-155 and Gd-157 are very large. As a result, in LEU assembly, they burn extremely quickly. However, due to the harder neutron spectrum in MOX assembly, Gd isotopes burn slowly. Gd-157 depletes faster in both assemblies than Gd-155, because of its larger absorption cross-section.

The isotopic concentrations for cell-1 are shown in Figs 6–13.

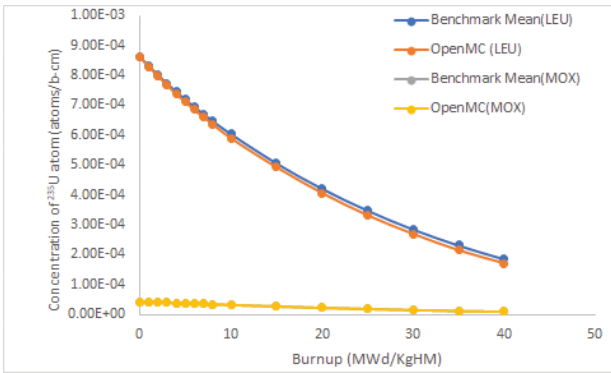


Figure 6. Variation of ^{235}U concentration vs burnup.

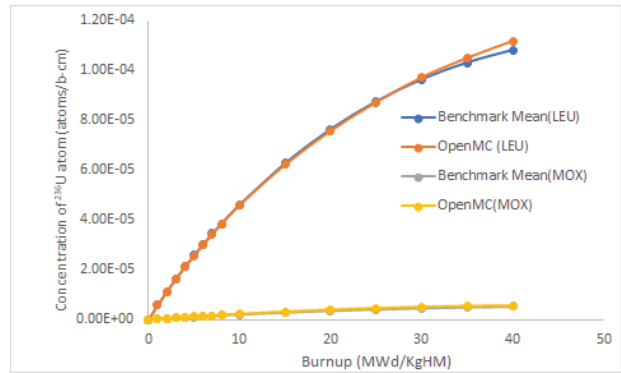


Figure 7. Variation of ^{236}U concentration vs burnup.

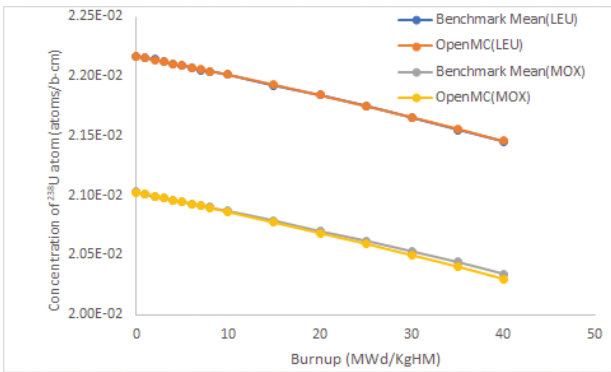


Figure 8. Variation of ^{238}U concentration vs burnup.

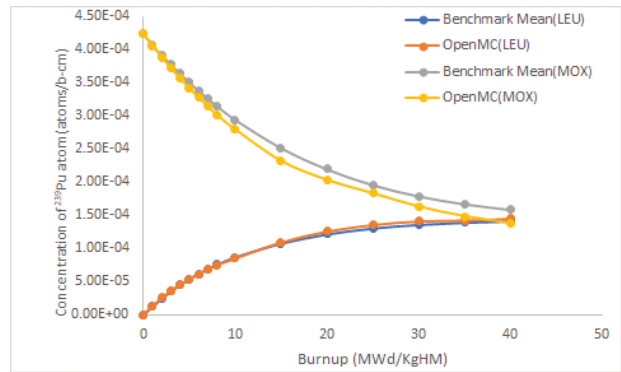


Figure 9. Variation of ^{239}Pu concentration vs burnup.

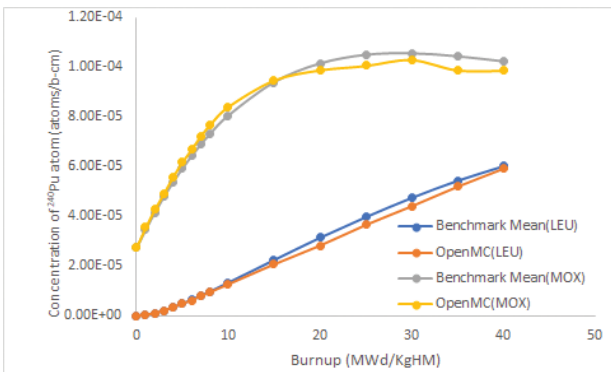


Figure 10. Variation of ^{240}Pu concentration vs burnup.

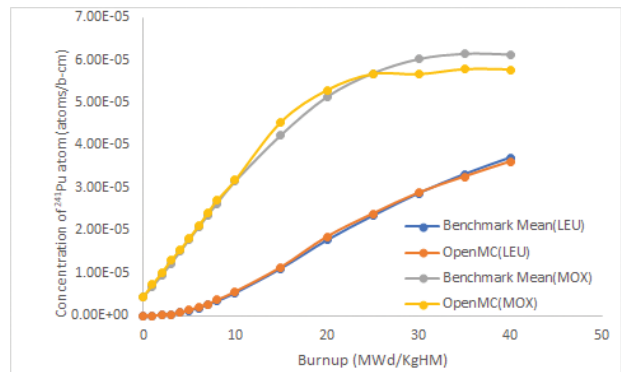


Figure 11. Variation of ^{241}Pu concentration vs burnup.

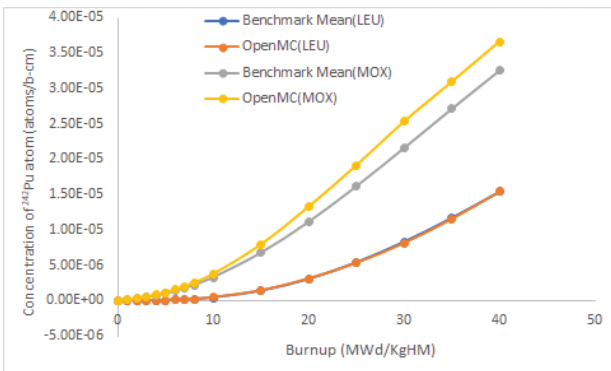


Figure 12. Variation of ^{242}Pu concentration vs burnup.

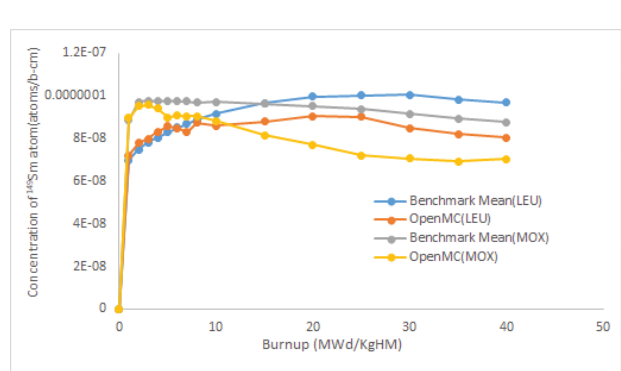


Figure 13. Variation of ^{149}Sm concentration vs burnup.

The isotopic concentrations for cell 24 are shown in Figs 14–23.

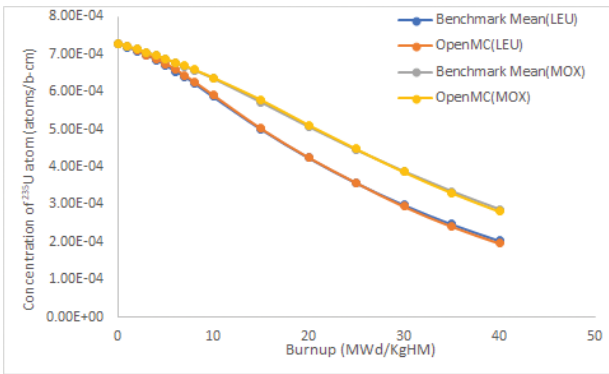


Figure 14. Variation of ^{235}U concentration vs burnup.

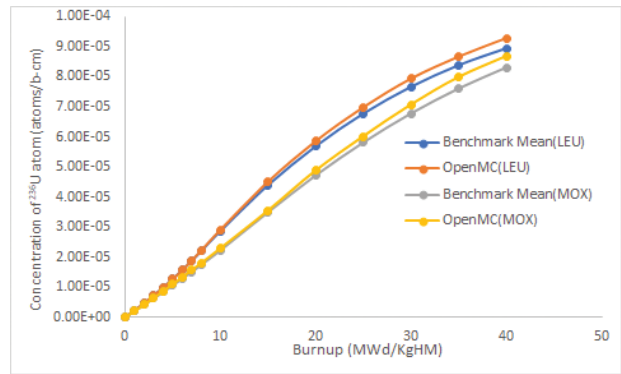


Figure 15. Variation of ^{236}U concentration vs burnup.

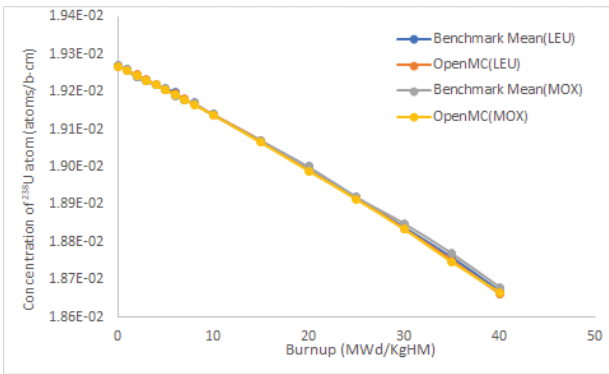


Figure 16. Variation of ^{238}U concentration vs burnup.

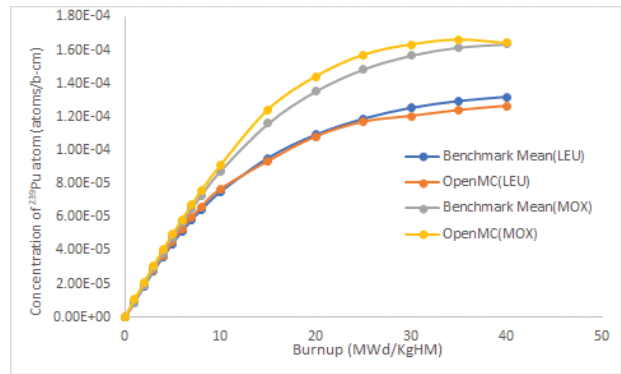


Figure 17. Variation of ^{239}Pu concentration vs burnup.

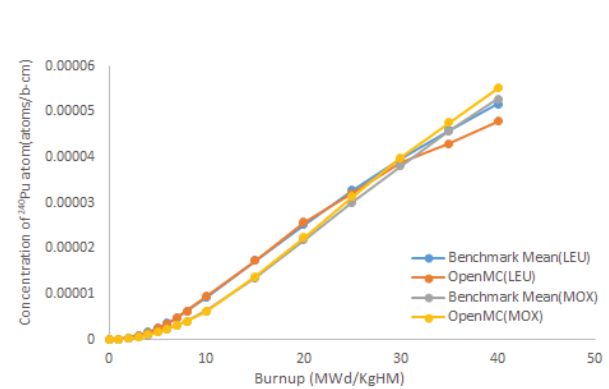


Figure 18. Variation of ^{240}Pu concentration vs burnup.

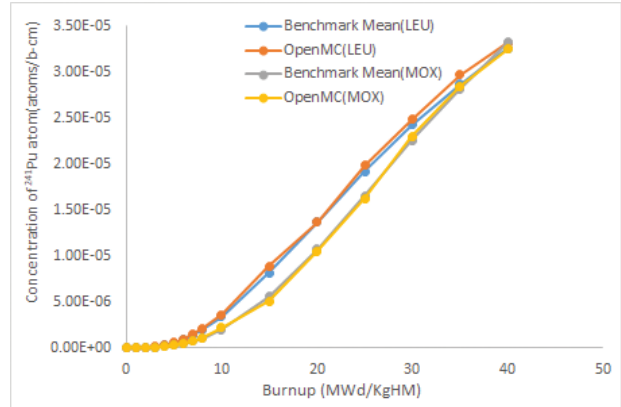


Figure 19. Variation of ^{241}Pu concentration vs burnup.

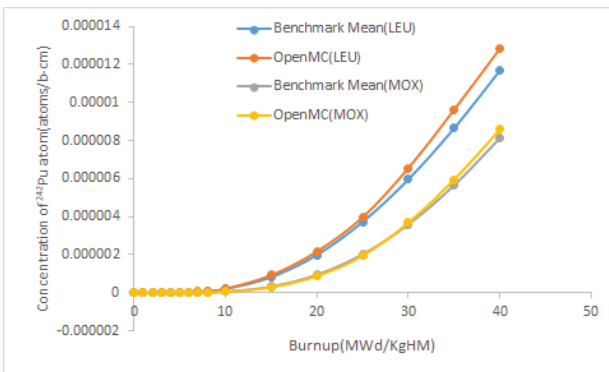


Figure 20. Variation of ^{242}Pu concentration vs burnup.

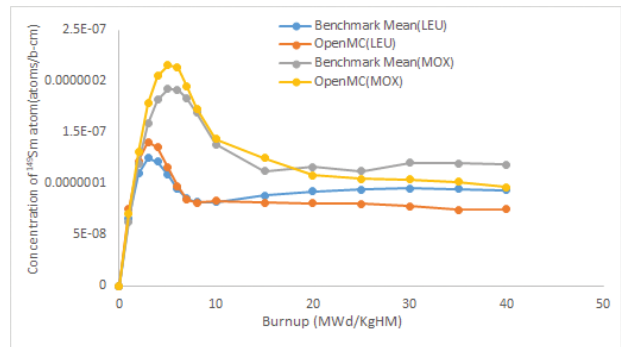


Figure 21. Variation of ^{149}Sm concentration vs burnup.

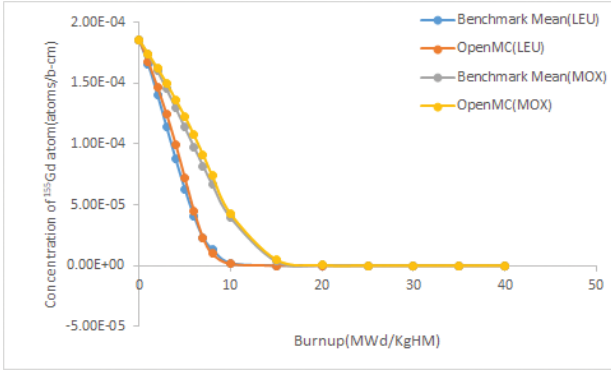


Figure 22. Variation of ^{155}Gd concentration vs burnup.

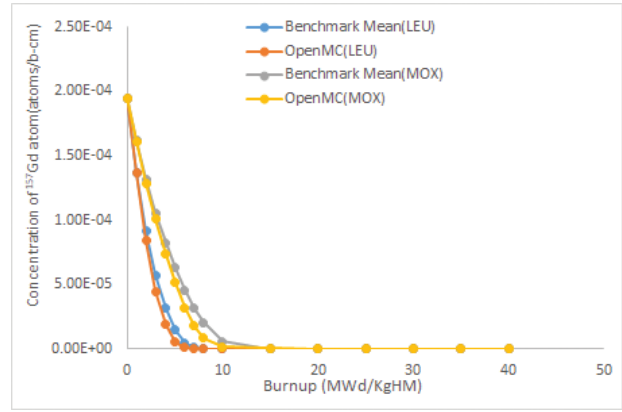


Figure 23. Variation of ^{157}Gd concentration vs burnup.

Assembly average concentration changes with burnup is shown in Figs 24–32.

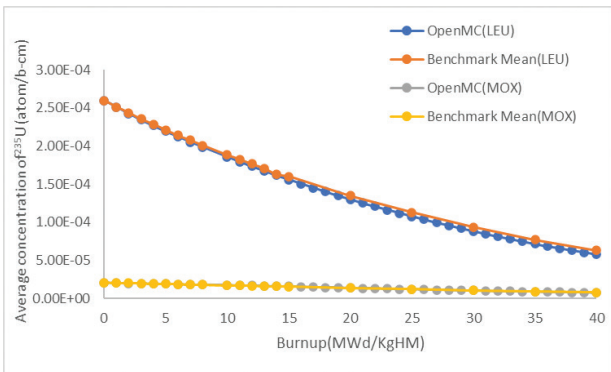


Figure 24. Variation of ^{235}U average concentration.

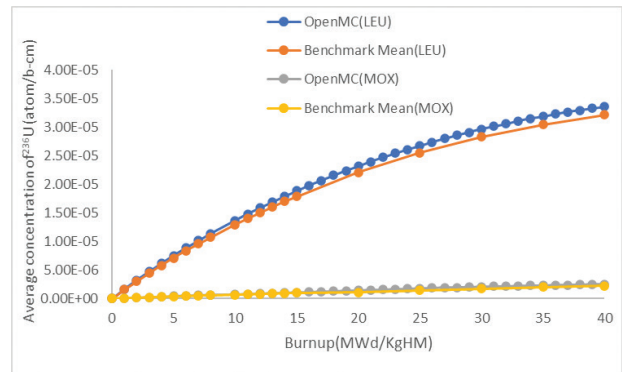


Figure 25. Variation of ^{236}U average concentration.

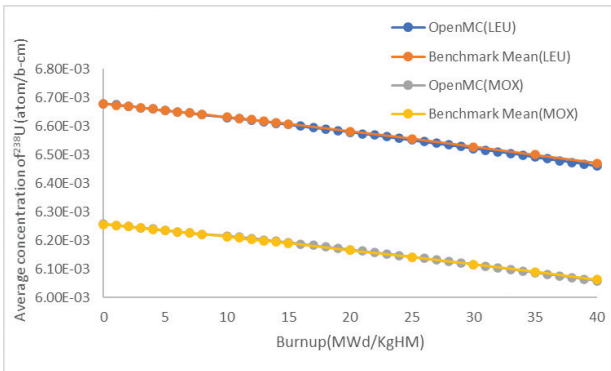


Figure 26. Variation of ^{238}U average concentration.

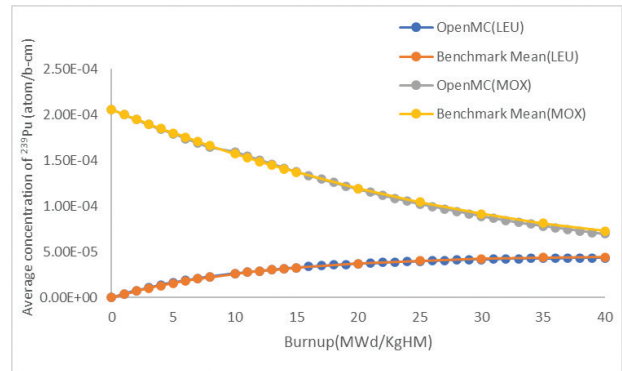


Figure 27. Variation of ^{239}Pu average concentration.

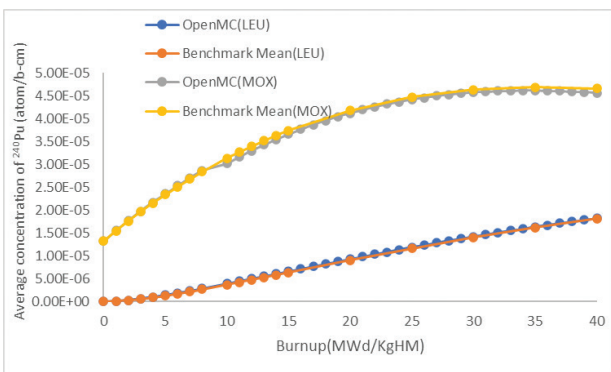


Figure 28. Variation of ^{240}Pu average concentration.

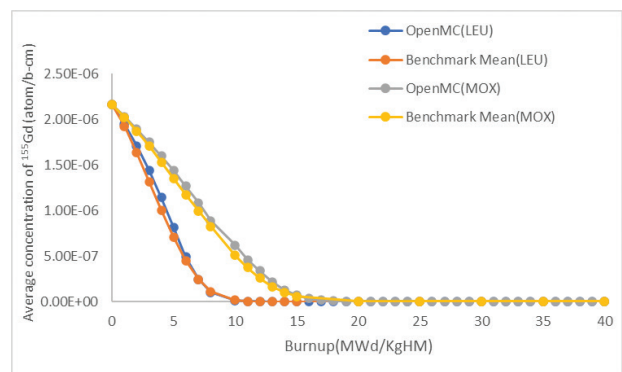


Figure 29. Variation of ^{155}Gd average concentration.

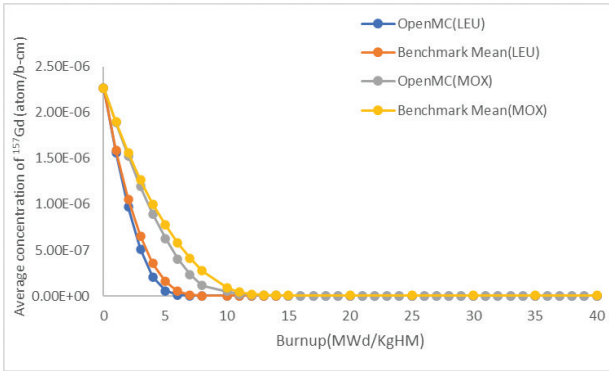


Figure 30. Variation of ¹⁵⁷Gd average concentration.

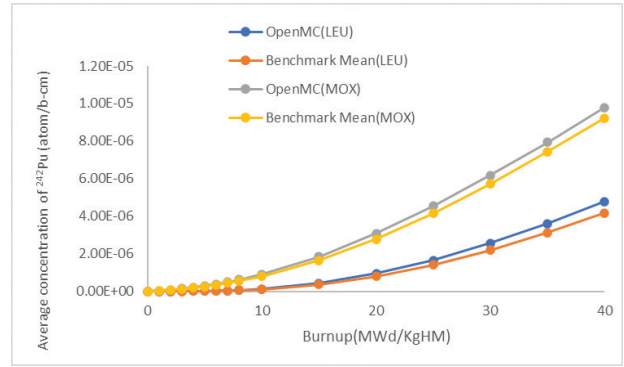


Figure 31. Variation of ²⁴²Pu average concentration.

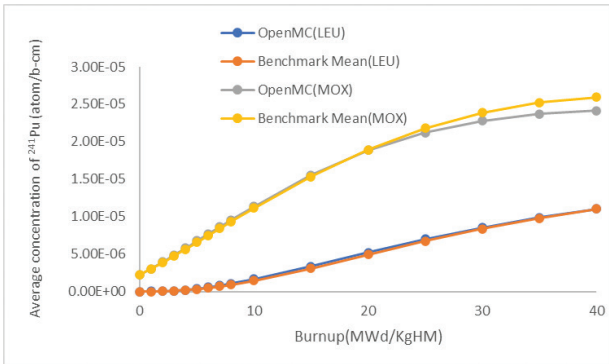
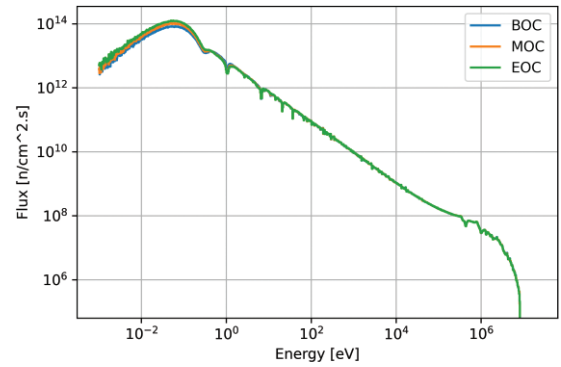
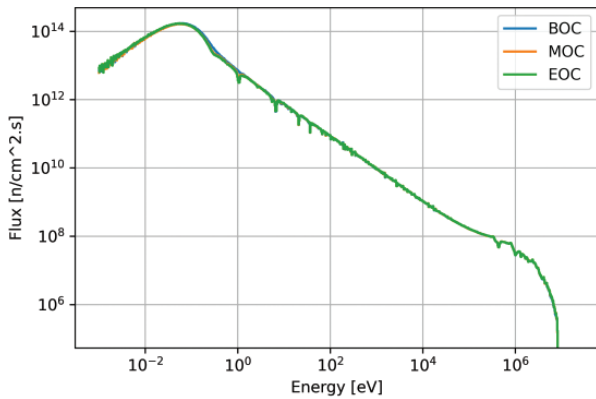


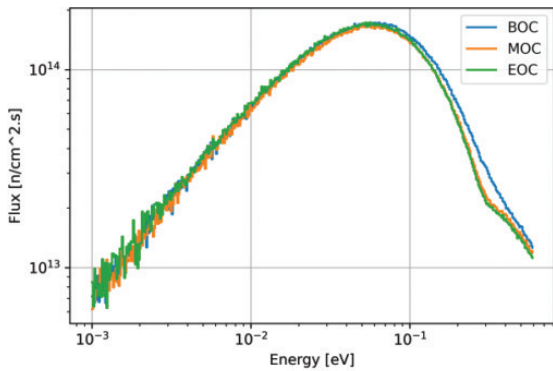
Figure 32. Variation of ²⁴¹Pu average concentration.



(a) Full energy spectrum

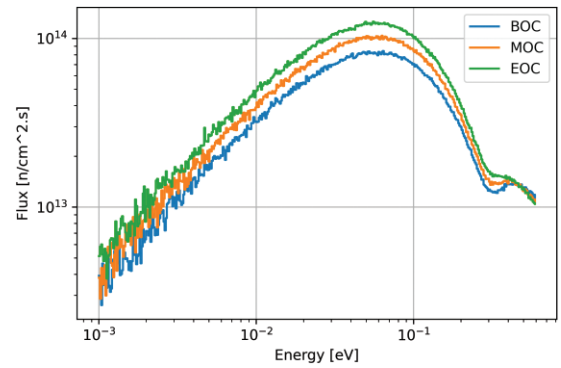


(a) Full energy spectrum



(b) Neutron energy spectrum for thermal energy region

Figure 33. Comparison of neutron flux spectrum at BOC, MOC and EOC for LEU fuel assembly.



(b) Neutron energy spectrum for thermal energy region

Figure 34. Comparison of neutron flux spectrum at BOC, MOC and EOC for MOX fuel assembly.

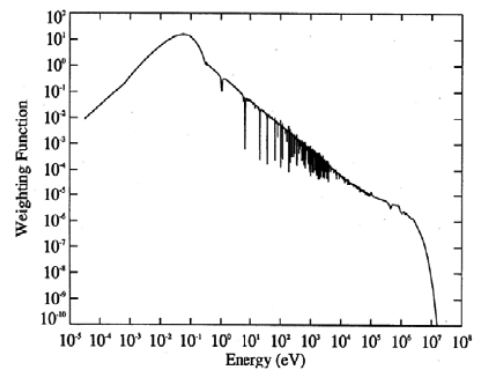


Figure 35. A typical neutron energy spectrum of a Light Water Reactor used as a weighting function in a generation of ORIGEN library [Tanaka et al. 2015].

Neutron flux distribution

Figs 33 and 34 present the neutron energy spectrum with respect to fluxes at three burnup cycles i.e. Beginning of Cycle (BOC), Middle of Cycle (MOC) and End of Cycle (EOC) for State-1 of LEU and MOX fuel assembly, respectively. The typical neutron energy spectrum is comprised of three kinds of spectra; thermal Maxwellian spectrum in thermal energy range, 1/E spectrum in epi-thermal energy range and fission spectrum in fast energy range. The shape of the typical spectrum has been given as results from neutron transport phenomena which are supposed to be observed in the LWR. Emitting neutrons by nuclear fission and moderation by light water are being considered in the phenomena for generation of such neutron energy spectrum (Figs 33 and 34). The neutron energy flux spectrum for each energy group has been calculated by dividing the neutron flux by the width of every energy group, $\phi(\text{cm}^{-2} \cdot \text{s}^{-1} \cdot \text{eV}^{-1}) = \Phi(\text{cm}^{-2} \cdot \text{s}^{-1})/\Delta E(\text{eV})$ by using OpenMC code. As may be seen from the Figs 33 and 34, good agreements are noticed between the neutron energy flux spectrum for BOC, MOC and EOC with slight variation among them especially MOX fuel assembly. No such neutron energy spectrum is available in the benchmark report to compare with OpenMC results. For comparison purpose, a typical neutron energy spectrum of a Light Water Reactor (Tanaka et al. 2015) is shown in Fig. 35. The neutron energy spectrum (Figs 33a and 34a) of VVER-1000 for State-1 (LEU and MOX fuel assembly) is almost identical shape of light water reactor (Fig. 3). Hence, the OpenMC code was successfully used for obtaining a neutron energy spectrum.

Conclusion

The k_{inf} values were calculated for VVER-1000 LEU & MOX assemblies that are typically of the advanced Russian designs in different reactor operating states using OpenMC code with nuclear data library ENDF/B-VII.1. The k_{inf} values were also calculated against fuel burnup

upto 40 MWd/kgHM. In addition, the isotope composition was also calculated for burnup upto 40 MWd/kgHM as per benchmark requirements. The calculated results were compared with the benchmark mean values along with the literature data. The OpenMC results showed very good agreement with the benchmark mean values along with other literature values. The neutron energy spectrum was successfully generated by using OpenMC code for both LEU and MOX fuel assembly for State-1. It is concluded that the OpenMC code along with the nuclear data library ENDF/B-VII.1 was successfully implemented at the Department of Nuclear Science and Engineering Department, MIST. In Bangladesh, two Russian design VVER-1200 (2400 MW_{th}) type nuclear reactors are under construction and to be commissioned by 2023/2024. Based on the experience achieved for implementation of OpenMC code in the field of neutronics and burnup calculations, it is planned to calculate k_{inf} or to perform burnup calculations for VVER-1200 and other PWR and BWR by using OpenMC along with SuperMC.

Authorship contribution statement

Md. Imtiaz Hossain: Methodology, Data collection, Formal analysis, Writing – original draft. Yasmin Akter: Resources, data analysis, writing. Mehraz Zaman Faridin: Resources, literature review, writing. A. S. Mollah: Supervision, Conceptualization, Results interpretation, Writing – review & editing.

Acknowledgements

The authors really acknowledge the efforts of the Department of Nuclear Science and Engineering, Military Institute of Science and Technology, Dhaka, Bangladesh for their academic support. The authors thank the referees for their critical reading of the paper and for the improvements they suggested.

References

- Abuqudaira TM, Stogov YV (2018) Neutronic calculations for the VVER-1000 LEU and MOX assembly computational benchmark using the GETERA code. *Journal of Physics: Conference Series* 1133: 012018. <https://doi.org/10.1088/1742-6596/1133/1/012018>
- Alhassan E, Sjostrand H, Duan J, Helgesson P, Pomp S, Osterlund M (2014) Selecting benchmarks for reactor calculations PHYSOR 2014, PHYSOR 2014 – The Role of Reactor Physics toward a Sustainable Future, The Westin Miyako, Kyoto, Japan, September 28–October 3, 2014, on CD-ROM.
- Aljassar SA, Naymushin AG, Aish MM (2021) Computational-benchmark analysis with the GETERA and serpent softwares tools for VVER fuel assemblies, *Journal of Jilin University (Engineering and Technology Edition)* 40: 09–2021.
- Brown FB (2006) On the Use of Shannon Entropy of the Fission Distribution for Assessing Convergence of Monte Carlo Criticality Calculations. *Proceedings PHYSOR-2006*, Vancouver, Canada, Sept 10–14.
- Brown FB, Kiedrowski B, Bull J (2010) MCNP5-1.60 Release Notes, LA-UR-10-06235, Los Alamos National Laboratory.
- Diop CM, Petit O, Dumonteil E, Hugot FX, Lee YK, Mazzolo A, Trama JC (2007) TRIPOLI-4: A 3D Continuous-Energy Monte Carlo Transport Code. *Proc. of the PHYTRA1: First International Conference on Physics and Technology of Reactors and Applications*, Marrakech, Morocco, Mar. 14–16, 2007, GMTR.
- ENDF/B-VII.1 (2012) Evaluated Nuclear Data File David Brown Presented at the 2012 ANS Winter Meeting Town & Country Hotel & Resort, San Diego, CA November 11–15.

- Isotalo AE, Leppänen J, Dufek J (2013) Preventing xenon oscillations in Monte Carlo burnup calculations by enforcing equilibrium xenon distribution. *Annals of Nuclear Energy* 60: 78–85. <https://doi.org/10.1016/j.anucene.2013.04.031>
- Jiankai Yu (2021) Nuclear physics probability code: OpenMC. In: *Nuclear Power Plant Design and Analysis Codes*, Woodhead Publishing Series in Energy, 123–138. <https://doi.org/10.1016/B978-0-12-818190-4.00006-1>
- Khan SA, Jagannathan V, Kannan U, Mathur A (2016) Study of VVER1000 OECD LEU & MOX computational benchmark with VISWAM Code system. *Nuclear Energy and Technology* 2(4): 312–334. <https://doi.org/10.1016/j.nucet.2016.11.008>
- Louis HK, Amin E (2016) The Effect of Burnup on Reactivity for VVER-1000 with MOXGD and UGD Fuel Assemblies Using MCNPX Code. *Journal of Nuclear and Particle Physics* 6(3): 61–71.
- Mercatali L, Beydogan N, Sanchez-Espinoza VH (2021) Simulation of low-enriched uranium burnup in Russian VVER-1000 reactors with the Serpent Monte-Carlo code. *Nuclear Engineering and Technology* 53: 2830–2838. <https://doi.org/10.1016/j.net.2021.03.014>
- Mercatali L, Venturini A, Daeubler M, Sanchez VH (2015) SCALE and SERPENT solutions of the OECD VVER-1000 LEU and MOX burnup computational benchmark. *Annals of Nuclear Energy* 83: 328–341. <https://doi.org/10.1016/j.anucene.2015.03.036>
- OECD NEA (2002) A VVER-1000 LEU and MOX Assembly Computational Benchmark, NEA/NSC/DOC(2002)10.
- Petrov N, Todorova G, Kolev NP (2013) APOLLO2 and TRIPO-LI4 solutions of the OECD VVER-1000 LEU and MOX assembly benchmark. *Annals of Nuclear Energy* 55: 93–107. <https://doi.org/10.1016/j.anucene.2012.12.010>
- Romano PK, Horelik NE, Herman BR, Nelson AG, Forget B, Smith K (2015) OpenMC: A State-of-the-Art Monte Carlo Code for Research and Development. *Annals of Nuclear Energy* 82: 90–97. <https://doi.org/10.1016/j.anucene.2014.07.048>
- Romano PK, Forget B (2013) The OpenMC Monte Carlo Particle Transport Code. *Annals of Nuclear Energy* 51: 274–281. <https://doi.org/10.1016/j.anucene.2012.06.040>
- Tanaka K-i, Ueno J, Adachi M, Chiba S (2015) Improvement of a calculation procedure of neutron-flux distribution for radioactivity inventory estimation for decommissioning of nuclear power plants. *Progress in Nuclear Energy* 85: 254–270. <https://doi.org/10.1016/j.pnucene.2015.05.009>
- Thilagam L, Sunil Sunny C, Jagannathan V, Subbaiah KV (2009) A VVER-1000 LEU and MOX assembly computational benchmark analysis using the lattice burnup code EXCEL. *Annals of Nuclear Energy* 36: 505–519. <https://doi.org/10.1016/j.anucene.2008.12.015>
- Wu Y, Song J, Zheng HQ (2015) CAD-based Monte Carlo program for integrated simulation of nuclear system SuperMC. *Annals of Nuclear Energy* 82: 161–168. <https://doi.org/10.1016/j.anucene.2014.08.058>